Contribution from the Department of Chemistry,
Southwest Texas State University, San Marcos, Texas 78666

Models for the Binding Site in Bromoperoxidase: Mononuclear Vanadium(V) Phenolate Complexes of the Hydridotris(3,5-dimethylpyrazolyl)borate Ligand

Stephen Holmes and Carl J. Carrano*

Received June 11, 1990

Vanadium (3,5-dimethylpyrazolyl)borate complexes with a series of phenolate ligands have been prepared and characterized. The single-crystal X-ray structure of the *p*-bromophenol derivative tris[(3,5-dimethylpyrazolylborato]bis(*p*-bromophenoxy)oxovanadium(V) has been determined by standard methods and refined to an unweighted *R* factor of 0.052. The dark green triclinic crystals belong to space group $P\bar{1}$ with cell dimensions of a = 12.140 (3) Å, b = 13.515 (4) Å, c = 10.811 (3) Å, α = 107.96 (2)°, β = 116.15 (2)°, and γ = 75.78 (3)°. Phenolate coordination stabilizes the V(V) oxidation state to the extent that the V(IV) complexes are easily air oxidized. Near linear correlations are observed between the Hammett σ constants for the para substituents on the phenoxy rings and physicochemical parameters such as LMCT band position and redox potentials. The phenoxy complexes also undergo relatively facile hydrolysis to produce the oxo-bridged dimer, $[LVO(OH)]_2O$. The implications of this work to the binding site model proposed for the V(V)-dependent bromoperoxidase enzyme from marine algae are discussed.

Introduction

Bromoperoxidases recently isolated from various species of marine algae represent the first-known vanadoenzymes.[1-4] These V(V)-dependent enzymes catalyze the oxidative bromination of a variety of organic substrates, according to the following equation:

$$RH + H_2O_2 + Br^- \rightarrow RBr + OH^- + H_2O$$

Based primarily on EPR and EXAFS data, a preliminary model of the binding site in these enzymes is now available.[5-7] Three of the ligands appear to be well established, two histidine nitrogens and a terminal oxo group. The remaining three donors are not known with certainty, but oxygens from tyrosine, serine, aspartic acid, or glutamic acid have been suggested.

In a previous communication, we reported a series of "half-sandwich" V(III) and V(IV) complexes with the (3,5-dimethylpyrazolyl)borate ligand, which we hoped might serve as models for the binding site in the bromoperoxidase enzymes.[8] The (3,5-dimethylpyrazolyl)borato group was chosen because of the similarity of its nitrogen donors with those of histidine. However, in order to serve as appropriate models it is necessary for the vanadium to be in the +5 oxidation state. Thus, we have begun to seek ways of stabilizing the $HB(Me_2pz)_3V^VO(X)(Y)$ unit by varying the identity of the ancillary ligands X and Y. We have shown in the past that the phenolate group is an excellent ligand for vanadium and can lead to stable complexes of the relatively rare VO^{3+} moiety.[9-11] In addition, the phenolic oxygens of tyrosine have been suggested as possible ligands in the native enzyme.[7] Therefore, we have explored the substitution chemistry of $LV^{IV}O(Cl)DMF$ with phenolate ligands and have found that stable V(V) complexes can indeed be formed. The results of these studies are reported herein and to our knowledge represent the first mononuclear V(V) complexes of the tris(3,5-dimethylpyrazolyl)borato ligand known. The implications of this work to the binding-site model proposed for bromoperoxidase are discussed.

Experimental Section

Materials. Unless otherwise stated, reactions were run under an atmosphere of pure dry nitrogen by utilizing standard Schlenk techniques. Solvents were dried with the appropriate reagents and were distilled under inert atmosphere. Potassium hydridotris(3,5-dimethylpyrazolyl)borate, $[HB(Me_2pz)_3]VO(Cl)DMF$ (I) and $[HB(Me_2pz)_3]VO(acac)$ (II) were all prepared as previously described.[8,12]

Synthesis. $[HB(Me_2pz)_3]VO(p\text{-bromophenoxide})_2$ (IIIa). To 1.5 g of $[HB(Me_2pz)_3]VO(Cl)DMF$ dissolved in 30 mL of warm degassed toluene was added a slurry of sodium *p*-bromophenoxide in toluene. The initially pale green solution darkened to a brown-yellow color and was stirred under an inert atmosphere overnight. The flask was then opened to the air, and stirring continued for another 12 h, during which time the solution became a deep green. The solvent was removed under vacuum and the residue subjected to silica gel column chromatography using methylene chloride as an eluant. The deep green band that eluted first from the column was collected and rotary evaporated. The residue was crystallized from methylene chloride/hexane to yield 0.644 g (30%) as near black crystals. Anal. Calcd for $C_{27}H_{30}N_6BVOBr_2$: C, 45.76; H, 4.24; N, 11.86. Found: C, 45.61; H, 4.18; N, 11.75. The *p*-methoxy (IIIb), *p*-*tert*-butyl (IIIc), *p*-nitro (IIId), and unsubstituted phenol (IIIe) complexes were obtained in a similar fashion and had satisfactory elemental analyses.

$[HB(Me_2pz)_3]VO(OH)]_2O$. A sample of IIIe was dissolved in 25 mL of moist acetonitrile. The solution was refluxed for 1 h, during which time the deep-green solution turned a dark red-brown. The solution was reduced in volume and allowed to stand at −20 °C overnight, producing a crop of fine red-brown crystals. Anal. Calcd for $C_{30}H_{46}N_{12}B_2V_2O_5 \cdot 3H_2O$: C, 43.27; H, 6.25; N, 20.19. Found: C, 42.98; H, 5.61; N, 20.05.

Physical Methods. Infrared spectra were obtained as KBr pellets on a Perkin-Elmer 1600 FT-IR. Optical measurements employed a Perkin-Elmer 553 spectrophotometer. Both ^1H and ^{13}C NMR spectra were recorded on an IBM/Bruker 80-MHz FT-NMR utilizing $CDCl_3$ as a solvent and are referenced to internal TMS. EPR spectra were obtained on a Brucker ER-300 instrument. Analyses were performed by Desert Analytics. Electrochemical data were obtained by using a BAS CV-27 and techniques previously described.[13,14] Cyclic voltammograms were run in Burdick & Jackson "distilled in glass" DMF, acetonitrile, or methylene chloride, containing 0.1 M tetrabutylammonium hexafluorophosphate as a supporting electrolyte. Potentials were referenced to a saturated calomel electrode (SCE) and an internal ferrocene standard. Optically transparent thin-layer electrochemical (OTTLE) data employed a homemade cell similar to that previously described.[14]

Collection and Analysis of X-ray Data. A data crystal of IIIa was obtained as described above, mounted in a Lindeman capillary and transferred to a Rigaku AFC6R diffractometer employing graphite-monochromated Cu Kα radiation and a 12-kW rotating anode generator. Cell constants and an orientation matrix were obtained from a least-squares refinement of 25 carefully centered reflections in the range of $67.2 < 2\theta < 79.64°$. Crystal data and collection parameters are summarized in Table I.

Solution and Refinement of Structure. Data were reduced and the models refined with the TEXSAN program package supplied by Molecular Structure Corp. On the basis of packing considerations, a statistical

(1) Vilter, H. *Phytochemistry* **1984**, *23*, 1387.
(2) Weber, R.; deBoer, E.; Plat, H.; Krenn, B. E. *FEBS Lett.* **1987**, *216*, 1.
(3) Plat, H.; Krenn, B. E.; Wever, R. *Biochem. J.* **1987**, *248*, 277.
(4) Krenn, B. E.; Plat, H.; Wever, R. *Biochim. Biophys. Acta* **1987**, *912*, 287.
(5) deBoer, E.; Boon, K.; Wever, R. *Biochemistry* **1988**, *27*, 1629.
(6) deBoer, E.; Keijzers, C. P.; Kaassen, A. A. K.; Reigerse, E. J.; Collison, D.; Garner, C. D.; Wever, R. *FEBS Lett.* **1988**, *235*, 93.
(7) Arber, J. M.; deBoer, E.; Garner, C. D.; Hasnain, S. S.; Wever, R. *Biochemistry* **1989**, *28*, 7968.
(8) Kime-Hunt, E.; Spartalian, K.; DeRusha, M.; Nunn, C. M.; Carrano, C. J. *Inorg. Chem.* **1989**, *28*, 4392.
(9) Bonadies, J. A.; Carrano, C. J. *J. Am. Chem. Soc.* **1986**, *108*, 4088.
(10) Bonadies, J. A.; Pecoraro, V. L.; Butler, W.; Carrano, C. J. *Inorg. Chem.* **1987**, *26*, 1218.
(11) Bonadies, J. A.; Carrano, C. J. *Inorg. Chem.* **1986**, *25*, 4358.
(12) Trofimenko, S. *J. Am. Chem. Soc.* **1967**, *89*, 6288.
(13) Marrese, C. A.; Carrano, C. J. *Inorg. Chem.* **1983**, *22*, 1858.
(14) Marrese, C. A.; Carrano, C. J. *Inorg. Chem.* **1984**, *23*, 3961.

0020-1669/91/1330-1231$02.50/0

Table I. Summary of Crystallographic Data and Data Collection

A. Crystal Data	
empirical formula	$C_{27}H_{30}N_6O_3Br_2VB$
fw	708.13
crystal color, habit	deep green, prism
crystal dimens	0.400 × 0.200 × 0.200 mm
crystal system	triclinic
no. of reflcns used for unit cell determination (2θ range)	25 (67.5–79.6°)
ω-scan peak width at half-height	0.27
lattice params	
a	12.140 (3) Å
b	13.515 (4) Å
c	10.811 (3) Å
α	107.96 (2)°
β	116.15 (2)°
γ	75.78 (3)°
V	1502.0 (8) Å^3
space group	$P\bar{1}$ (No. 2)
Z	2
D_{calc}	1.566 g/cm^3
F_{000}	712
μ(Cu Kα)	62.57 cm^{-1}
B. Intensity Measurements	
diffractometer	Rigaku AFC5R
radiation	Cu Kα (λ = 1.541 78 Å)
temp	23 °C
attenuators	Zr foil (factors: 3.6, 12.3, 44.7)
take-off angle	6.0°
detector aperture	6.0 mm horizontal 6.0 mm vertical
crystal to detector dist	40 cm
scan type	ω–2θ
scan rate	32.0°/min (in ω) (2 rescans)
scan width	(1.26 ± 0.30 tan θ)°
$2\theta_{max}$	120.1°
no. of reflcns measured	total, 4712 unique, 4468 (R_{int} = 0.071)
correcns	Lorentz–polarization absorption (transm factors 0.59–1.00) secondary extinction (coeff 0.183 32 × 10^{-5})
C. Structure Solution and Refinement	
structure solution	direct methods
refinement	full-matrix least-squares
function minimized	$\sum w(\|F_o\| - \|F_c\|)^2$
least-squares weights	$4F_o^2/\sigma^2(F_o^2)$
p factor	0.02
anomalous dispersion	all non-hydrogen atoms
no. of observations ($I > 3.00\sigma(I)$)	2718
no. of variables	362
reflcn/param ratio	7.51
goodness of fit indicator	2.00
residuals: *R*; R_w	0.052; 0.056
max shift/error in final cycle	0.01
max peak in final diff map	0.61 e/Å^3
min peak in final diff map	−0.77 e/Å^3

analysis of the intensity distribution, and the successful solution and refinement of the structure, the space group was determined to be $P\bar{1}$. The structure was solved by using the direct methods program, SHELXS of George Sheldrick, and refined by using full-matrix least-squares refinement. Hydrogen atoms located on a difference map were not refined but included as fixed contributions at idealized positions. Parameters used in the solution and refinement of the structure are included in Table I. Final atomic positional parameters are found in Table II.

Results and Discussion

Oxidation of [HB(Me$_2$pz)$_3$]VO(acac). Our initial attempt to produce stable V(V) complexes with pyrazolylborate ligands involved electrochemical oxidation of previously prepared V(IV) species. [HB(Me$_2$pz)$_3$]VO(acac) was chosen over [HB(Me$_2$pz)$_3$]VO(Cl)DMF as the redox potential of the latter was near the oxidative limit of the solvent. A cyclic voltammogram of [HB(Me$_2$pz)$_3$]VO(acac) in methylene chloride is shown in Figure 1. Bulk electrolysis on a Pt basket electrode at +1.3 V

Table II. Positional Parameters and *B*(eq) for IIIA

atom	*x*	*y*	*z*	*B*(eq), Å^2
Br(1)	1.2588 (1)	0.0902 (1)	0.6894 (1)	10.16 (7)
Br(2)	0.5032 (1)	−0.1819 (1)	−0.3835 (2)	12.93 (8)
V(1)	0.8027 (1)	0.31213 (9)	0.0875 (1)	3.59 (5)
O(1)	0.7544 (4)	0.1832 (3)	0.0382 (5)	4.4 (2)
O(2)	0.9716 (4)	0.2750 (3)	0.1793 (4)	4.0 (2)
O(3)	0.7705 (4)	0.3579 (3)	0.2225 (5)	4.5 (2)
N(1)	0.6239 (5)	0.3579 (4)	−0.0575 (5)	3.8 (2)
N(2)	0.6044 (5)	0.4020 (4)	−0.1651 (5)	3.7 (2)
N(3)	0.8334 (5)	0.4566 (4)	0.0844 (6)	3.5 (2)
N(4)	0.7954 (5)	0.4895 (4)	−0.0381 (6)	3.6 (2)
N(5)	).8508 (5)	0.2626 (4)	−0.1094 (6)	3.9 (2)
N(6)	0.7927 (5)	0.3186 (4)	−0.2126 (6)	3.7 (2)
C(1)	0.5123 (6)	0.3490 (5)	−0.0676 (7)	4.1 (3)
C(2)	0.4223 (6)	0.3872 (6)	−0.1827 (8)	4.8 (3)
C(3)	0.4820 (6)	0.4199 (5)	−0.2418 (7)	4.2 (3)
C(4)	0.4943 (6)	0.3060 (6)	0.0330 (8)	5.3 (4)
C(5)	0.4274 (7)	0.4652 (6)	−0.3693 (8)	5.9 (4)
C(6)	0.8970 (6)	0.5210 (6)	0.1899 (8)	4.3 (3)
C(7)	0.9001 (6)	0.6085 (6)	0.1352 (9)	4.8 (3)
C(8)	0.8365 (6)	0.5825 (5)	−0.0067 (8)	4.3 (3)
C(9)	0.9517 (7)	0.5232 (6)	0.3398 (8)	5.5 (4)
C(10)	0.8130 (7)	0.6374 (6)	−0.1171 (9)	6.0 (4)
C(11)	0.9132 (6)	0.1767 (5)	−0.1609 (8)	4.3 (3)
C(12)	0.8942 (7)	0.1762 (6)	−0.2971 (8)	5.1 (4)
C(13)	0.8188 (6)	0.2667 (6)	−0.3265 (7)	4.2 (3)
C(14)	0.9890 (8)	0.0951 (6)	−0.079 (1)	6.4 (4)
C(15)	0.7713 (7)	0.3097 (6)	−0.4558 (8)	5.7 (4)
C(16)	0.6973 (6)	0.1039 (5)	−0.0594 (8)	4.2 (3)
C(17)	0.6621 (8)	0.0920 (7)	−0.202 (1)	6.1 (4)
C(18)	0.6060 (9)	0.0066 (8)	−0.297 (1)	7.8 (5)
C(19)	0.5838 (8)	−0.0674 (7)	−0.250 (1)	7.5 (4)
C(20)	0.6142 (9)	−0.0542 (7)	−0.111 (1)	7.3 (5)
C(21)	0.6719 (7)	0.0288 (6)	−0.0144 (9)	5.7 (4)
C(22)	1.0324 (6)	0.2355 (5)	0.2949 (7)	3.8 (3)
C(23)	1.1565 (7)	0.2461 (6)	0.3748 (8)	5.7 (4)
C(24)	1.2226 (7)	0.2045 (7)	0.4908 (9)	6.3 (4)
C(25)	1.1672 (8)	0.1505 (6)	0.5307 (8)	5.8 (4)
C(26)	1.0454 (8)	0.1368 (6)	0.4516 (9)	5.8 (4)
C(27)	0.9774 (6)	0.1805 (6)	0.3366 (8)	4.9 (4)
B(1)	0.7161 (7)	0.4233 (6)	−0.1805 (9)	3.9 (4)

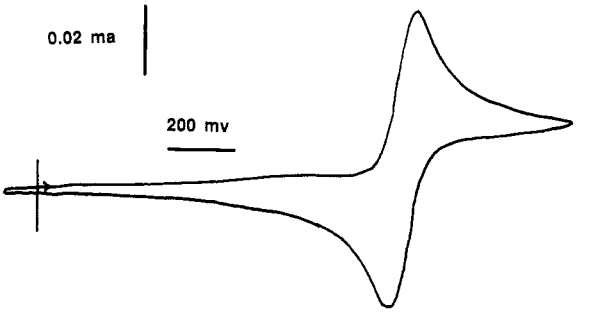

Figure 1. Cyclic voltammograph at a Pt bead electrode of a ca. 2 mM solution of [HB(Me$_2$pz)$_3$]V^{IV}O(acac) in methylene chloride containing 0.1 M tetrabutylammonium hexafluorophosphate (TBAPF$_6$). Scan rate: 200 mV/s.

in methylene chloride consumed 0.96 electrons/mol and gave a deep blue solution. The process was reversible if undertaken quickly, with reelectrolysis at 0.0 V regenerating the starting complex. However, it was noted that the deep blue color of the oxidized material began to fade over the course of several tens of minutes, suggesting that the V(V) product produced was unstable and underwent decomposition. Accurate UV–visible spectral data were therefore recorded with an OTTLE cell attached to a Perkin-Elmer 553 spectrophotometer, which allowed rapid spectral monitoring of the oxidation product. Stepping the potential of a gold minigrid between +1.0 and +1.3 V in 50-mV increments resulted in an increasing absorbance at ~695 nm. Above +1.3 V, no further increases were noted. A spectrum of the deep blue V(V) product is shown in Figure 2. Three bands are seen at ~350, 530, and 695 nm (ϵ_m = 2070). The magnitude of the extinction coefficient and the fact that V(V) is a d^0 system

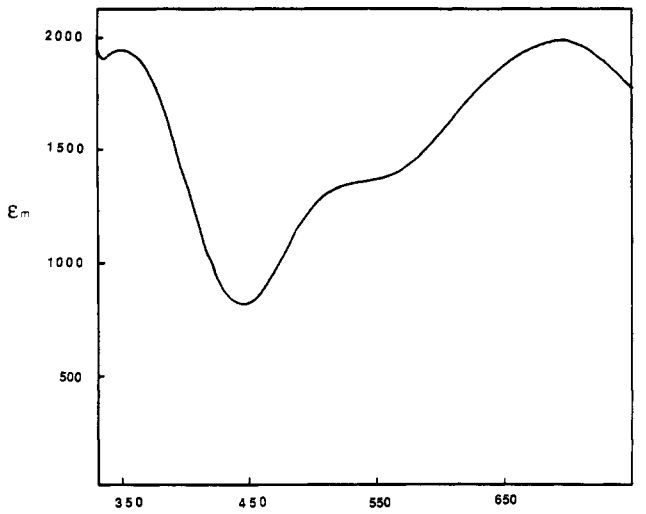

Figure 2. Optical spectrum of $[HB(Me_2pz)_3]V^V(acac)$ in 0.1 M $TBAPF_6$ containing acetonitrile solution, obtained via electrolysis at a gold minigrid in an OTTLE cell, as described in the text.

indicates clearly that the optical bands are LMCT in character. The deep blue color and corresponding optical spectrum is characteristic of oxovanadium(V) coordinated to good π-donating ligands such as a phenoxide or acac.[9] Despite the fact that a V(V) complex could be prepared by direct oxidation of a V(IV) species, its instability indicated that another approach was needed.

Synthesis and Characterization of V(V) Phenolates. In an attempt to increase the stability of the relatively electron deficient V(V) center, we sought to replace the acac ligand in II with a better π-donating moiety. For this role we chose the phenolate group. As expected, the reaction of a sodium or lithium phenoxide salt with $LV^{IV}O(Cl)DMF$ resulted in the formation of a V(IV) phenoxide complex by replacement of the chloride ligand. The complex was not isolated, but an EPR spectrum was recorded. It was noted that solutions of these V(IV) complexes became deeply colored and lost their EPR signal when exposed to air, suggesting oxidation to the d^0 V(V). The overall reaction is

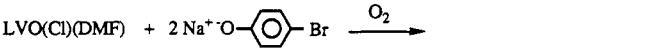

The V(V) species were purified by column chromatography on silica gel using methylene chloride as an eluant. The desired complexes were eluted rapidly as deep green to blue bands. Further purification was achieved by recrystallization from hexane or methylene chloride/hexane solutions. The fact that all the V(V) para-substituted phenoxy complexes were soluble in nonpolar solvents including hydrocarbons indicated that they were uncharged materials. All complexes displayed a B–H stretch at $\sim$2530 cm^{-1} and the single aromatic C–N band at 1542 cm^{-1} indicative of a tris-coordinated pyrazolylborate group.[8] A $\nu_{V=O}$ was observed in all complexes at 950–960 cm^{-1} as were bands assignable to the phenoxy ligands at 1475 cm^{-1} ($\nu_{C=C}$), 1240 cm^{-1} (ν_{C-O}), and 860 cm^{-1} (ring mode). Proton NMR spectra of the complexes in $CDCl_3$ provided unambiguous information as to the structure of these complexes in solution.

The free pyrazolylborate ligand in DMSO-d_6 shows a single peak at $\sim$5.5 ppm due to the lone C–H proton on the three equivalent pyrazolyl rings, as well as ones at 2.09 and 2.01 ppm due to the inequivalent ("up" vs "down") methyl resonances. All the compounds in this study show a more complex NMR pattern. The ring C–H proton resonance is split into two peaks at $\sim$5.7 and 5.6 ppm in a 2:1 ratio, indicating that the pyrazolylborate rings are now inequivalent with two being of one type and one unique. The methyl resonances are also split, again in a 2:1 ratio, with the up and down methyls on the two equivalent rings found at $\sim$2.40 and 2.35 ppm, a splitting similar to that seen in the free ligand, with the corresponding methyls on the unique ring appearing at $\sim$2.40 and $\sim$1.72 ppm. The phenyl protons of the para-substituted derivatives also show the expected A_2B_2 pattern centered around 7 ppm. Substituent protons, i.e. the *tert*-butyl methyls and methoxy methyls also appear in characteristic positions. NMR data for all the complexes prepared are summarized in Table III. The NMR data just presented argues for the presence of a plane of symmetry in the molecule. A reasonable structure that possesses such a mirror plane and that is consistent with the other physicochemical data has two phenoxides replacing the chloride and DMF in the starting material leading to a neutral V(V) complex. In this structure the up methyls on the pyrazolylborate rings are expected to experience nearly the same environment in III as in the free ligand and thus appear at a similar chemical shift. The down methyls on the two equivalent rings in III sandwich the oxo group and therefore also appear at a chemical shift similar to that in the free ligand. However, the down methyl on the unique ring is sandwiched between the two phenolate groups and thus experiences a considerable ring current anisotropy that pushes this resonance upfield from its position in the free ligand. The solution structure just described has been verified in the solid state by a single-crystal X-ray diffraction analysis.

Table III. NMR Data for Vanadium(V) Bisphenolate Complexes (ppm from TMS)

complex	aromatic	pyrazolyl ring		methyl		substituent
p-methoxy	6.90	5.73	5.66	2.39	2.35	3.78
				2.39	1.91	
p-*tert*-butyl	7.13	5.72	5.66	2.39	2.33	1.30
				2.42	1.92	
p-H	7.02	5.75	5.63	2.41	2.35	
				2.41	1.83	
p-bromo	7.02	5.77	5.61	2.41	2.35	
				2.41	1.72	
p-nitro	7.42	5.83	5.58	2.45	2.38	
				2.45	1.57	

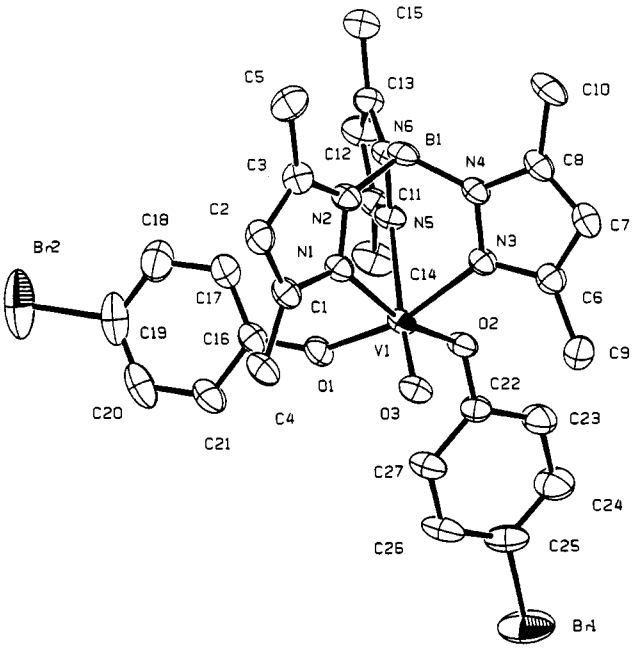

Figure 3. Structure of $[HB(Me_2pz)_3]VO(p\text{-bromophenoxide})_2$, showing 50% probability thermal ellipsoids and the atom labeling scheme.

Description of Structure. As expected, the solution structure as determined by NMR is similar to that found in the solid state by X-ray diffraction. Complex IIIa is a mononuclear V(V) complex containing a facially coordinating tridentate (3,5-dimethylpyrazolyl)borate ligand. Two *p*-bromophenoxide ligands and an oxo group complete the pseudoctahedral geometry. The overall structure and atom labeling scheme are shown in Figure 3. Relevant bond lengths and angles are found in Table IV. The

Table IV. Selected Bond Lengths (Å) and Angles (deg) for IIIa

V(1)–O(1)	1.822 (4)	V(1)–N(1)	2.119 (5)
V(1)–O(2)	1.857 (4)	V(1)–N(3)	2.088 (5)
V(1)–O(3)	1.579 (4)	V(1)–N(5)	2.311 (5)
O(1)–V(1)–O(2)	98.0 (2)	O(2)–V(1)–N(5)	82.6 (2)
O(1)–V(1)–O(3)	97.5 (2)	O(3)–V(1)–N(1)	95.1 (2)
O(1)–V(1)–N(1)	86.8 (2)	O(3)–V(1)–N(3)	94.1 (2)
O(1)–V(1)–N(3)	164.3 (2)	O(3)–V(1)–N(5)	174.2 (2)
O(1)–V(1)–N(5)	88.1 (2)	N(1)–V(1)–N(3)	81.6 (2)
O(2)–V(1)–O(3)	98.1 (2)	N(1)–V(1)–N(5)	83.6 (2)
O(2)–V(1)–N(1)	165.1 (2)	N(3)–V(1)–N(5)	80.1 (2)
O(2)–V(1)–N(3)	90.7 (2)		

Table V. Optical Spectral Data for Vanadium(V) Bisphenolate Complexes

complex	λ_{max}, nm (ϵ_m)		
p-methoxy	400 (4000)	570 (4425)	800 (4540)
p-*tert*-butyl	400 (5930)	530 (5810)	740 (6017)
p-bromo	390 (6837)	590 (5725)	700 (6175)
p-H	400 (5270)	570 (4230)	675 (4460)
p-nitro		550 (9200)	630 (8750)

N–V–N angles are all less than the idealized 90° (average 81.8°) due to the "bite" of the pyrazolylborate group. The vanadium(V)–oxo bond length is 1.58 Å while the two vanadium(V)–phenoxy oxygen bonds average 1.89 (1) Å. The vanadium–nitrogen bond trans to the oxo group is, as expected from the trans effect, considerably longer (2.31 vs 2.10 Å) than the other two bonds. The remaining bond lengths and angles are unremarkable. A comparison of vanadium complexes in oxidation states ranging from +II to +V with pyrazolylborate ligands shows the expected trend toward shorter V–N bond lengths with increasing oxidation state, although the differences are not large.[15] More significant perhaps is the shortening of the V=O bond from 1.65 Å in the V(IV) starting material to 1.58 Å in IIIa.

Spectroscopic and Electrochemical Properties. All of the V(V) complexes in this study are highly colored with complicated optical spectra (Table V). Generally three bands are seen with extinction coefficients in the 4000–8000 M^{-1} cm^{-1} range, leading to blue to green coloration. The magnitude of the extinction coefficients and the lack of d electrons on V(V) suggests that these must be either LMCT or internal π–π^* transitions. LMCT transitions are characteristic of the VO^{3+} moiety with phenolate ligation.[9] The position of the lowest energy band is highly sensitive to the nature of the substituent in the para position of the coordinated phenoxy group, and therefore it seems reasonable to assign this as a LMCT transition, since electron-withdrawing groups are expected to lower the energy of the phenolate oxygen π orbitals resulting in an increasing ligand to metal energy gap. As expected, there is a near linear correlation between energy of the LMCT transition and Hammett σ constants (Figure 4). The fact that the highest energy band (~400 nm) is relatively unaffected by the nature of X suggests that it is an intraligand transition. It is difficult to detect any trends in the intermediate energy band due to extensive overlaps with the other transitions.

Redox potentials for the complexes were also measured by cyclic voltammetry. All the complexes showed quasi-reversible electrochemical behavior (i.e. $i_{pa}/i_{pc} \approx 1$ and peak to peak separation similar to that of the known reversible one-electron standard ferrocene). The redox potentials also show the same trends with changes in the substituents on the phenoxy ligands, as do the optical spectra. As can be seen in Table VI, the redox potentials can be tuned over at least a 600-mV range just by varying the para substituent on the phenoxy ring. The strongly electron withdrawing *p*-nitro derivative is the easiest to reduce while the electron releasing *p*-methoxy is the hardest. Between the most electron releasing phenolate complex and the starting $[HB(Me_2pz)_3]V^{IV}O(Cl)DMF$ there is an over 1.5-V stabilization of

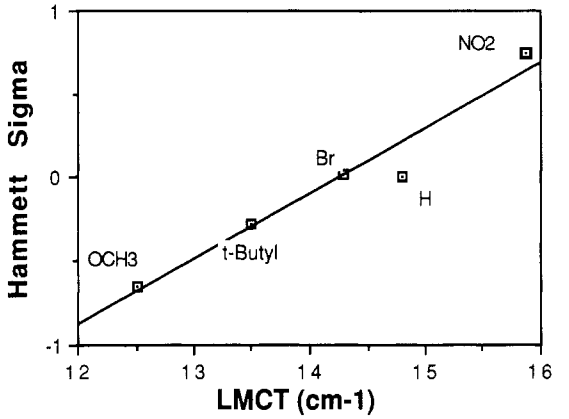

Figure 4. Plot of Hammet σ constant for para substituent, X, on the phenoxy rings of $[HB(Me_2pz)_3]V^V(p\text{-}OC_6H_4X)_2$ complexes vs lowest energy LMCT band position (in thousands of wavenumbers). The line represents the best least-squares fit and has a correlation coefficient of 0.944.

Table VI. Redox Potentials of $[HB(Me_3pz)_3]VO(X)(Y)$ Complexes

complex (X, Y)	$E°$(vs SCE), V
I (Cl, DMF)	+1.43
II (acac)	+1.18
IIId (*p*-nitrophenoxy)	+0.510
IIIa (*p*-bromophenoxy)	+0.155
IIIe (phenoxy)	−0.040
IIIc (*p*-*tert*-butylphenoxy)	−0.070
IIIb (*p*-methoxyphenoxy)	−0.125

V(V) over V(IV), clearly showing the oxophilicity of the higher oxidation state. Although we have not done a complete study, these same trends are observed in the ^{51}V NMR spectra of these complexes, which show shifts ranging from −484 ppm (relative to $VOCl_3$) for the most electron donating *p*-methoxyphenol to −588 ppm for the strongly electron withdrawing *p*-nitro derivative.

Reaction Chemistry. In attempts to prepare single crystals suitable for X-ray diffraction analysis, the unsubstituted phenoxy derivative was recrystallized from acetonitrile. During the attempted recrystallization it was noted that the deep green color of the starting complex suddenly changed to red brown. From this solution a red brown crystalline solid was subsequently isolated. IR analysis of the product showed the expected "tris" pyrazolylborato bands at 2522 and 1542 cm^{-1}, as well as a V=O stretch at 966 cm^{-1}; however the bands attributed to the coordinated phenolates at 1475, 1240, and 857 cm^{-1} had disappeared. The only new band to appear was a strong one at 785 cm^{-1}, assigned as a V–O–V asymmetric stretch.[16] The diamagnetism of the solid and the presence of an unshifted NMR spectrum in DMSO-d_6 indicated that the vanadium was still in the +5 oxidation state. Only three peaks were seen in the NMR, centered at 5.72 ppm (s, C–H on pyrazolyl ring), 2.11 (d, up and down methyls on pyrazolyl ring), and 3.29 (broad, OH), confirming the loss of the phenolate groups. The peak at 3.29 ppm was determined to be an OH via its exchangeability with D_2O. On the basis of these data, as well as elemental analysis, we believe that the red product is the dimeric oxo-bridged $[LVO(OH)]_2O$ formed from hydrolysis and dimerization of the starting phenolate complexes in wet acetonitrile, according to the following equation:

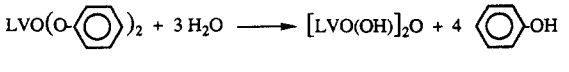

The structure of a related complex, where L = 1,4,7-trimethyl-1,4,7-triazacyclononane, has recently been determined by Weighardt and co-workers.[15] The optical spectrum of the product displays a strong band of ~470 nm (ϵ_m = 460), assignable as a

(15) V(II)–N (part a), 2.17 Å; V(III)–N (part b), 2.13 Å; V(IV)–N (part b), 2.11; V(V)–N (part c), 2.10: (a) Dapporto, P.; Mani, F.; Mealli, C. *Inorg. Chem.* **1978**, *17*, 1323. (b) Reference 8. (c) This work.

(16) Knopp, P.; Wieghardt, K.; Nuber, B.; Weiss, J.; Sheldrick, W. S. *Inorg. Chem.* **1990**, *29*, 363.

LMCT transition probably arising from the following moiety.

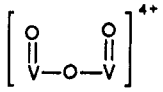

Similar LMCT bands have been observed in other complexes containing this group.[17]

Implications for the V(V) Binding Site in the Bromoperoxidases. From the recent EXAFS data it now appears likely that the V(V) in native bromoperoxidase finds itself in a distorted octahedral environment consisting of two histidine nitrogens at ~2.11 Å, a terminal oxo group at 1.61 Å, and approximately three other light atom donors at ~1.72 Å. The reduced form of the enzyme is similar but has a slightly longer V=O bond distance of 1.63 Å and a considerably longer vanadium–light atom bond length of 1.91 Å. It has been speculated that one or more of the light atom donors in the bromoperoxidases might arise from the phenolate oxygens of a tyrosine. Other possible ligands include deprotonated serine alkoxo oxygens or carboxylates from glutamic or aspartic acid.

The V(V) phenoxy complexes of the trispyrazolylborate group prepared in this work have a donor set remarkably similar to that implicated in the bromoperoxidase enzyme, and we believe the data presented in this report, along with work previously published, both by our group and others, will allow us to *eliminate* tyrosine as a ligand in the native enzyme. The data suggesting this are two-fold. First and perhaps foremost is that we have found, without exception, that the VO^{3+} moiety coordinated to one or more phenolate donors invariably leads to intense LMCT transitions in the visible region of the optical spectrum. These bands appear without regard to the nature of the ancillary ligands, whether the complex is 5 or 6 coordinate, or whether the phenols are chelated or not.[9-11] These LMCT bands, typically with extinction coefficients of 2000–4000 M^{-1} cm^{-1} per coordinated phenolate group, give rise to deep green to violet colors, *which should be present in the enzyme if tyrosine were a ligand but clearly are not.*[18,19] Second, oxovanadium(V) phenolate bond lengths found in the literature and including those reported in this work average 1.87 Å, considerably longer than the 1.72 Å suggested by the EXAFS data for the native enzyme.[10,17,20,21] If we therefore eliminate tyrosine as a likely ligand, we are left with the deprotonated alkoxy oxygen of a serine residue or a mono- or bidentate carboxylato group from aspartic or glutamic acids. A brief survey of the literature reveals that both mono- and bidentate carboxylate oxygen to oxovanadium(V) moieties average ~2.0 Å,[22] while alkoxo oxygens average ~1.78 Å.[20,21,23] The short bond length seen with the alkoxides is believed to be due to considerable multiple-bond character in this interaction (1.99 Å expected for a V–O single bond based on sum of the ionic radii). The good π donation of the alkoxide oxygens also leads to a considerable stabilization of the electron-poor V(V) oxidation state and substitutes in many ways for a terminal oxo group. An equally possible alternative is that the donors at 1.72 Å do not come from the protein at all but represent protonated oxo groups, i.e. V–OH. There is considerable precedence for the protonation of terminal oxo groups on V(V) at physiologically accessible pH values.[9,16] Weighardt's recent structural characterization of the complex $[L_2V_2O_4(\mu\text{-}O)]$ and its protonated analogue $[L_2V_2O_2(OH)_2(\mu\text{-}O)]^{2+}$ where L = 1,4,7-trimethyl-1,4,7-triazacyclononane has shown that the 1.65-Å terminal V=O bond lengthens to ~1.78 Å upon protonation.[16] This is in the same range as the V–O bond in alkoxy complexes. It thus seems clear that the most likely candidates for the additional light atom donors in the bromoperoxidase are either deprotonated serine hydroxyls or protonated terminal oxo groups. We are presently investigating the optical and other physicochemical properties of these types of coordination with V(V).

Acknowledgment. This work is supported in part by grants from the Robert A. Welch Foundation, No. AI-1157, and the Research Corp. We thank Drs. Jan Troup and Paul Swetston of the Molecular Structure Corp. for assistance with the collection and solution of the X-ray structure. We also thank Prof. Alison Butler and Roger DelaRosa, University of California—Santa Barbara, for obtaining the ^{51}V NMR spectra.

Supplementary Material Available: Tables S1–S4, listing positional parameters, complete bond lengths and angles involving non-hydrogen atoms, and anisotropic thermal parameters, and Table S6, listing analytical data (10 pages); a table of observed and calculated structure factors (30 pages). Ordering information is given on any current masthead page.

(17) Carrano, C. J.; Nunn, C. M.; Quan, R.; Bonadies, J. A.; Pecoraro, V. L. *Inorg. Chem.* **1990**, *29*, 944.
(18) de Boer, E.; Tromp, M. G. M.; Plat, H.; Krenn, G. E.; Wever, R. *Biochim. Biophys. Acta* **1986**, *872*, 104.
(19) de Boer, E.; Van Kooyk, Y.; Tromp, M. G. M.; Plat, H.; Wever, R. *Biochim. Biophys. Acta* **1986**, *869*, 48.
(20) Diamantis, A. A.; Fredericksen, J. M.; Salam, A.; Snow, M. R.; Tienkink, E. R. T. *Aust. J. Chem.* **1986**, *39*, 1081.
(21) Dutton, J. C.; Murray, K. S.; Tiekink, E. R. T. *Inorg. Chim. Acta* **1989**, *166*, 5.
(22) Rehder, D.; Priebsch, W.; Oeynhausen, M. *Angew. Chem., Int. Ed. Engl.* **1989**, *28*, 1221.
(23) Giacomelli, A.; Floriani, C.; Ofirde Souza Duarte, A.; Chiesi-Villa, A.; Guastini, C. *Inorg. Chem.* **1982**, *21*, 3310.